scientific reports

Check for updates

OPEN

In vitro antioxidant and antibacterial activities of biogenic synthesized zinc oxide nanoparticles using leaf extract of *Mallotus philippinensis* Mull. Arg

Arun Kumar Khajuria[1], Anuj Kandwal[2]✉, R. K. Sharma[1], Rakesh Kumar Bachheti[3,4,5], Limenew Abate Worku[6]✉ & Archana Bachheti[7]

The preparation of metallic nanoparticles (NPs) using the green method is rapid, eco-friendly, and easily scaled up at room temperature and pressure. In the current study, zinc oxide nanoparticles (ZnO NPs) were prepared utilizing leaf extract from *Mallotus philippinensis*, employing two distinct precursors of zinc oxide: zinc acetate and zinc nitrate. The antioxidant and antibacterial properties of the synthesized nanoparticles were also evaluated. The synthesis of ZnO NPs was preliminary monitored by UV–visible analysis. The biosynthesized nanoparticles were further characterized using a variety of techniques, such as Fourier transform infrared spectroscopy (FTIR), X-ray diffraction (XRD), transmission electron microscopy (TEM), and ultraviolet-visible (UV-Vis) spectroscopy. XRD peaks showed that nanoparticles synthesized from both zinc precursors exhibit crystalline properties, having wurtzite hexagonal shapes. The TEM analysis indicates that the average crystallite size was determined to be 21 nm and 28 nm for zinc nitrate and zinc acetate as precursor. FTIR analysis confirmed the presence of polyphenolic compounds on the surface of the nanoparticles, which likely acted as reducing and capping agents during ZnO NP synthesis. The antioxidant activity of *M. philippinensis*-mediated ZnO NPs was assessed in vitro. ZnO NPs synthesized using zinc nitrate exhibited higher antioxidant potential (IC_{50} = 65.31 µg/ml) compared to those synthesized using zinc acetate (IC_{50} = 66.87 µg/ml). Furthermore, the ZnO NPs demonstrated significant antibacterial activity against both gram-positive and gram-negative bacteria, including *Klebsiella pneumoniae* (*K. pneumoniae*), *Staphylococcus aureus* (*S. aureus*), *Escherichia coli* (*E. coli*), and *Streptococcus pneumoniae* (*S. pneumoniae*). The highest antibacterial activity was observed against *S. pneumoniae*, with a zone of inhibition of 14.97 ± 0.38 mm for ZnO NPs synthesized using zinc nitrate. These findings suggest that *M. philippinensis* leaf extract is an effective reducing and capping agent for the biosynthesis of ZnO NPs. The resulting nanoparticles exhibit potent antioxidant and antibacterial properties, highlighting their potential applications in biomedical and environmental fields.

Keywords Zinc oxide, Nanoparticles, XRD, Crystalline, FTIR, TEM, Antioxidant, Antimicrobial activity

In the twenty-first century, one of the most significant areas of research and development is nanotechnology and nanopharmacology, which examines the size and manipulation of matter at the atomic level, often between 1 and 100 nanometers[1–4]. In nanoforms, the surface-to-area volume ratio rises due to decreasing material size;

[1]Department of Botany, Cluster University Jammu, Jammu, Jammu and Kashmir 184001, India. [2]Department of Chemistry, Harsh Vidya Mandir (PG) College, Raisi, Haridwar, Uttarakhand, India. [3]Department of Industrial Chemistry, College of Natural and Applied Sciences, Addis Ababa Sciences and Technology University, P.O. Box-16417, Addis Ababa, Ethiopia. [4]Department of Allied Sciences, Graphic Era Hill University, Clement Town, Society Area, Dehradun, Uttarakhand 248002, India. [5]University Centre for Research and Development, Chandigarh University, Mohali 140413, India. [6]Department of Chemistry, College of Natural and Computational Science, Debre Tabor University, Debre Tabor, Ethiopia. [7]Department of Environmental Science, Graphic Era (Deemed to be University), Dehradun, Uttarakhand 248002, India. ✉email: anujkandwal4@gmail.com; limenewabate@gmail.com

this property makes the surface effects more noticeable and simpler to investigate[5,6]. Because of their superior physico-chemical and biological properties over bulk materials, nanomaterials have enormous potential in many scientific domains[7]. High surface-to-volume ratios are a distinctive characteristic of nanoparticles (NPs)[8]; larger surface areas and larger surface-to-volume ratios generally increase the reactivity of nanomaterials due to the larger reaction surface[9], which means that they are more appropriate candidates for pharmacological activities[10]. Nanopharmacology deals with the formulations at the nano level to treat different ailments with enhanced effects and minimum side effects[11].

Among the large variety of NPs available, Because of their unique physical, chemical, and biological characteristics, such as their solubility, chemical stability, and adhesiveness, metal oxide (MO) nanoparticles are seen as the most promising[12]. The use of hazardous substances in the reduction and capping processes of the MO NPs production results in a host of negative consequences for the environment, living systems, and flora. Synthesis of MO NPs using plant extract is non-toxic, inexpensive, environmentally compatible, and simple. Compared to classical chemicals, the resultant particles are also biocompatible and free of toxic stabilizers. Plant extracts contain a variety of active biomolecules that aid in the reduction and stabilize NPs[13].

Physical, chemical, and biological techniques can be used to synthesize nanomaterials. However, physical and chemical techniques use a higher temperature, more energy, and environmentally dangerous organic solvents such as sodium borohydride and hydrazine as reducing agents[12]. In light of this, the green chemistry subject has received more attention from researchers. The use of inexpensive materials, solvents that do not harm the environment, and non-toxic compounds are very important in the censer of green chemistry. The primary benefit of this approach was reduced processing time, environmental friendliness, and ease of handling. Additionally, in place of chemical reducing agents, bio-functional groups such as fibers, carbohydrates, polyphenols, proteins, and lipids work as capping and reducing agents for nanoparticle synthesis[14,15].

The number of diseases with microbial origins has increased in the modern era, and due to the advent of new infectious diseases and the development of harmful bacteria's resistance to present medications, it is imperative to find new options. Since plant-based materials are typically affordable and safe, developing new alternatives by employing phytochemicals to lessen losses[16,17] is interesting. Along with infectious diseases, diseases caused by oxidative stress induced by reactive oxygen species are a serious threat to humanity from an economic and social point of view[18,19]. The use of plant-based antioxidants and bioactive compounds such as flavonoids and polyphenols has been effective in the prevention of these diseases, and several studies have shown that these compounds possess antimutagenic, anticarcinogenic, antimicrobial, and antiviral activities[20]. These plant-based antioxidant or antibacterial agents are important to various industrial sectors, including healthcare, food, packaging, and the environment[21].

Due to their different use in the biological, medical, electronics, communications, sensors, UV-protective cosmetics, water purification, and cosmetics industries, MO NPs have attracted much interest from researchers point of view[22,23]. Recently, ZnO, CuO, Ag_2O, Fe_2O_3, CaO, NiO, and MgO NPs have received the most attention in the literature as having antibacterial action[24]. Among those NPs, ZnO is considered a prospective contender in biomedicine, particularly for antibacterial, antioxidant, anti-inflammatory, anticancer, and anti-diabetes applications[25]. The properties of ZnO-NPs have been investigated in a wide range of targeted applications, including electrical properties, antibacterial activity, antifungal activity, catalytic activity, and cosmetic industry[26]. Recently, green synthesized ZnO nanoparticles using plant extracts have been effectively used against multi-drug resistant microbes. Moreover, ZnO nanoparticles antioxidant properties using several plants extracts have also been reported[27]. For instance, Shnawa et al.(2023)[28] evaluate the antibacterial and antioxidant properties of aqueous *Ziziphus spina-christi* leaf extract-mediated zinc oxide nanoparticles. The result confirmed that the produced ZnO-NPs effectively affected the antibacterial properties against the tested microorganisms in a concentration-dependent manner. In another study, without modifying their structural characteristics, *Celosia argentea* mediated ZnO NPs enhanced the antioxidant and antibacterial activities[29]. *Pluchea indica* leaf extract was used to biosynthesize ZnO NPs to assess their antibacterial activity. The result indicated higher antibacterial activities against tested organisms[30].

M. philippinensis Muell. Arg (Euphorbiaceae), commonly known as Kamala, Sindur, Rohini, and Kambhal, is a small to medium-sized monoecious tree. The plant is well known for its medicinal potency and is used in both codified and non-codified systems of medicine. Ethnobotanically, the plant treats intestinal worms, wound healing, burns, oral contraceptives, and purgative[31–33]. In ethnoveterinary, plants treat Threadworms and Ascaris[34], and fruits are also considered antihelminthic. Besides this, the plant also has wide pharmacological preference, and it is known for its antibacterial activity, antifungal[35,36], antioxidant[36,37], anti-filarial[38], anti-fertility[39], antidiabetic[40], anti-leukemic[41], anti-HIV[42], anti-tumor[43], anti-tuberculosis[44], anti-inflammatory[45] and hepatoprotective[46] activities. However, no study on *M. philippinensis*-mediated ZnO NPs focuses on different ZnO sources for antioxidant and antibacterial activities. The synthesis of nanoparticles using green approaches is gaining unique importance due to its low cost, biocompatibility, high productivity, purity, and being environmentally friendly. So, the current study focused on the green synthesis of zinc oxide nanoparticles (ZnO-NPs) using two zinc precursors (zinc acetate and zinc nitrate) and leaf extracts from *M. philippinensis* for testing antioxidant and antibacterial potential. The prepared nanoparticles were assayed by the DPPH method for antioxidant potential and the well diffusion method for antibacterial potential.

Materials and methods

Plant collection

M. philippinensis leaves were collated from Indora, Himachal Pradesh, India's District Kangra. The collection of this plant material complied with the relevant institutional, national, and international guidelines and legislation. For collection of *M. philippinensis* plant species permissions or licenses were obtained from the Agricultural center of Jammu. The plant was officially identified by Nitin Katoch at the Department of Botany, University of

Jammu, India, where it was assigned the accession number HBJU16545 after the specimen was submitted. After gathering the healthy leaves, they were adequately cleaned using tap water to remove any remaining soil. After washing, the leaves were allowed to air dry for 15 to 20 days. Using a mortar and pestle, the dried leaf components were ground into a fine powder and placed in a container without air for later usage at room temperature.

Preparation of plant extract

8 g of finely produced *M. philippinensis* leave powder were soaked in 100 milliliters of distilled water in a conical flask, and the flask was then heated to a continuous 60 ºC on a hotplate for 10 min. The mouth of the flask was airtight with aluminum foil. After letting it cool to room temperature, Whatman filter paper number 1 was used to filter it. The extract's final volume was calculated to be 100 milliliters and kept at room temperature for further analysis.

Preliminary investigation of bioactive compounds in plant extract

Test of saponins

Mix 5 ml of distilled water with crude ethanol extract in a test tube to test for Saponins, shaking vigorously. If stable foam begins to form, saponins are present.

Test of terpenoids

To test for Terpenoids, mix 2 ml of ethanolic crude extract with 2 ml of chloroform and allow it to dehydrate. Then, add 2 ml of concentrated H_2SO_4 and heat it for 2 min. A grayish hue indicates the presence of terpenoids.

Test of flavonoids

Alkaline reagent test: A bright yellow color appeared when 2 milliliters of a 2% NaOH solution were added to an ethanol crude extract. Upon the addition of diluted acid droplets, the solution became colorless, indicating the presence of flavonoids.

Test of phenol

The addition of 2 milliliters of a 2% $FeCl_3$ solution to the ethanolic crude extract produced green or blue-black colors, indicating the presence of phenols.

Test of tannins

The combination of 2 milliliters of a 2% $FeCl_3$ solution with the ethanolic crude extract produced a green or blue-black hue, indicating the presence of tannins.

Test of steroids

Two milliliters of ethanolic crude extract, concentrated H_2SO_4, and chloroform are introduced simultaneously. The red coloration observed in the bottom chloroform layer indicated the presence of steroids.

Test of alkaloids

Mayer's reagent was added after combining 2 milliliters of 1% HCl with the C_2H_5OH crude extract and heating the mixture uniformly. The turbidity of the resultant precipitate was taken as evidence of the presence of alkaloids.

Test of glycosidase

The Keller-Killani test involves mixing an ethanolic crude extract with 2 milliliters of glacial acetic acid containing one or two drops of a 2% $FeCl_3$ solution. Next, fill a second test tube with the mixture and add 2 milliliters of concentrated H_2SO_4. The production of brown rings indicates the presence of cardiac glycosides.

Biofabrication zinc oxide nanoparticles

Biofabrication of ZnO NPs was carried out using two different samples. For one sample, 50 milliliters of *M. philippinensis* extract and 50 milliliters of 100 mM zinc acetate dehydrate were combined in a 1 to 1 ratio. In a second sample, 50 milliliters of 100 mM zinc nitrate and 50 milliliters of *M. philippinensis* extract were combined in a 1:1 ratio to create two distinct ZnO nanoparticles, as previously mentioned[3]. The reactions were allowed at 60 C for 4 h while continuously stirring using a magnetic stirrer. The precipitates formed in the reaction were collected by centrifuging at 4000 rpm after completion. The reaction mixtures take 24 h to settle down to form a pellet. After collecting the pellets, they were cleaned three times using double-distilled water and then dried in an oven set at 60 ºC for ten hours. After using a mill and pestle to homogenize the powdered nanoparticles, they were finally gathered in airtight vials for later usage. Figure 1 shows the synthesis of ZnO NPs using *M. philippinensis.*

Characterization of nanoparticles

UV–vis absorption

Visual markers (color change) were used to characterize produced nanoparticles in the preliminary stages. Utilizing a UV–Vis spectrophotometer, the optical properties of MB suspension were measured between 200 and 800 nm.

Transmission electron microscopic (TEM) study

The powder particles were analyzed at an accelerating voltage of 200 kV using Transmission Electron Microscopy (TEM) at a resolution of approximately 1 Å. To perform this investigation, we used a probe sonicator to dissolve

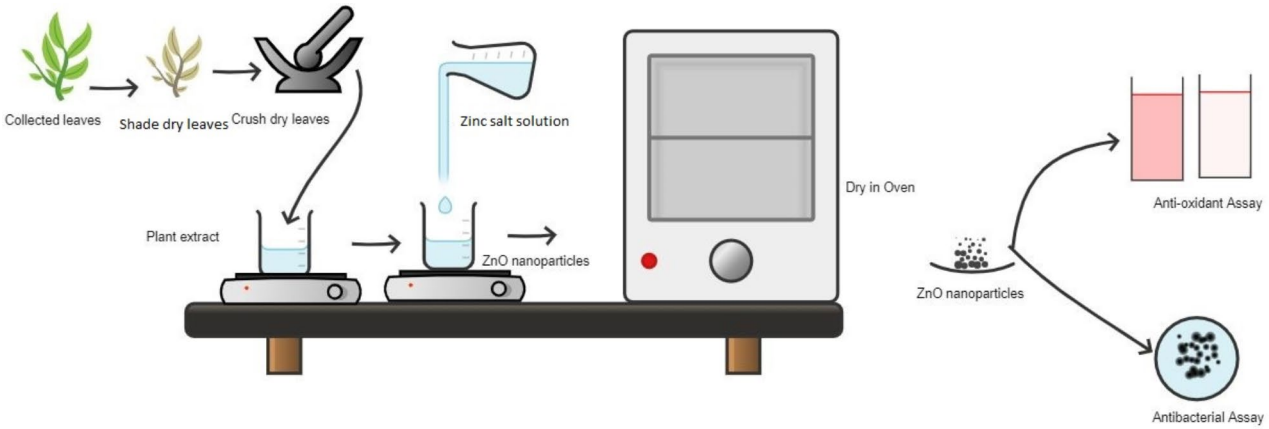

Fig. 1. Pictorial representation for the synthesis of ZnO NPs via *M. philippinensis*.

the ZnO sample in TDW. Then, TEM characterization was done after a drop of the combination was put into a carbon-coated copper grid and left to dry at room temperature.

Fourier transform infrared spectroscopy (FTIR)
An FTIR spectrometer was used to obtain the samples' FTIR spectra, which were recorded using a 400–4000 cm^{-1} wavenumber range. An IS50 FTIR spectrometer was used to conduct FTIR analysis.

X-ray diffraction (XRD)
XRD diffractometer was used to evaluate the crystallite size and shape of two ZnO NPs formed from Zinc nitrate and zinc acetate using monochromatic Cu Ka radiation at k = 1.54056 Aº in the 2-θ range of 5-80º. We used the Scherrer equation, often known as Eq. 1, to determine the crystallinity size[47].

$$\text{Crystalline size } (D) = \frac{k\lambda}{\beta\, cos\theta} \tag{1}$$

Where: D is the size of a crystallite in Å, θ is the scattering angle in radians, the wavelength of X-ray radiation is represented by λ (1.54178 Aº), Scherer's constant k has a value of 0.9, and the integral breadth of the maximum full width (FWHM) is represented by β.

Antioxidant activity

DPPH (2,2-diphenyl-1-picrylhydrazyl) free radical assay (Fig. 2) was performed to analysis the antioxidant potential of synthesized nanoparticles based on the methods used by Blois[48] and Desmarchelier et al.[49]. The alcoholic solution of DPPH was mixed with a substance having the potential of donating hydrogen atom resulting in reduced DPPH and loss of colour from purple to light yellow. Hence, 2 ml of a freshly prepared methanolic solution (0.1 Mm) of DPPH was mixed with 2 ml of (25, 75, 100 and 125 µg) solution of the ZnO-NPs. The test tubes were then left in the dark for 30 min. At 517 nm, the absorbance was measured following incubation. As a reference or control, ascorbic acid with concentration between 25 and 125 µg was used. A lower absorbance of the reaction mixture during measurement indicates a higher level of free radical scavenging activity[50]. Equation 2 was utilized to assess the antioxidant qualities of the samples by calculating the DPPH radical scavenging properties using ascorbic acid as a benchmark.

$$\text{SCV } (\%) = \frac{(\text{AC} - \text{AS})}{\text{AC}} \times 100 \tag{2}$$

where, AC and AS are absorbance of control and sample, SCV is the radical scavenging activity.

Antibacterial assay

The antibacterial activity of the generated nanoparticles was evaluated using the agar well diffusion method against gram-negative and gram-positive bacteria species, including *K. pneumoniae* and *E. coli*, as well as gram-positive bacteria, such as *S. aureus* and *S. pneumonia* (Fig. 2).

To prepare the Muller Hinton Agar Medium (HI-Media), 33.9 gram was dissolved in 1000 ml of purified water for the bacterial experiment. The dissolved medium was autoclaved for 15 min at 121 ºC and 15 Pa pressure. The media that had been autoclaved was subsequently transferred into a 20 × 90 mm Borosil petri plate situated beneath the laminar airflow chamber. Throughout the process, measures were taken to prevent any vapor production. A bacteriological incubator was used to incubate the prepared plates for 24 h at 30 ºC to look for contamination.

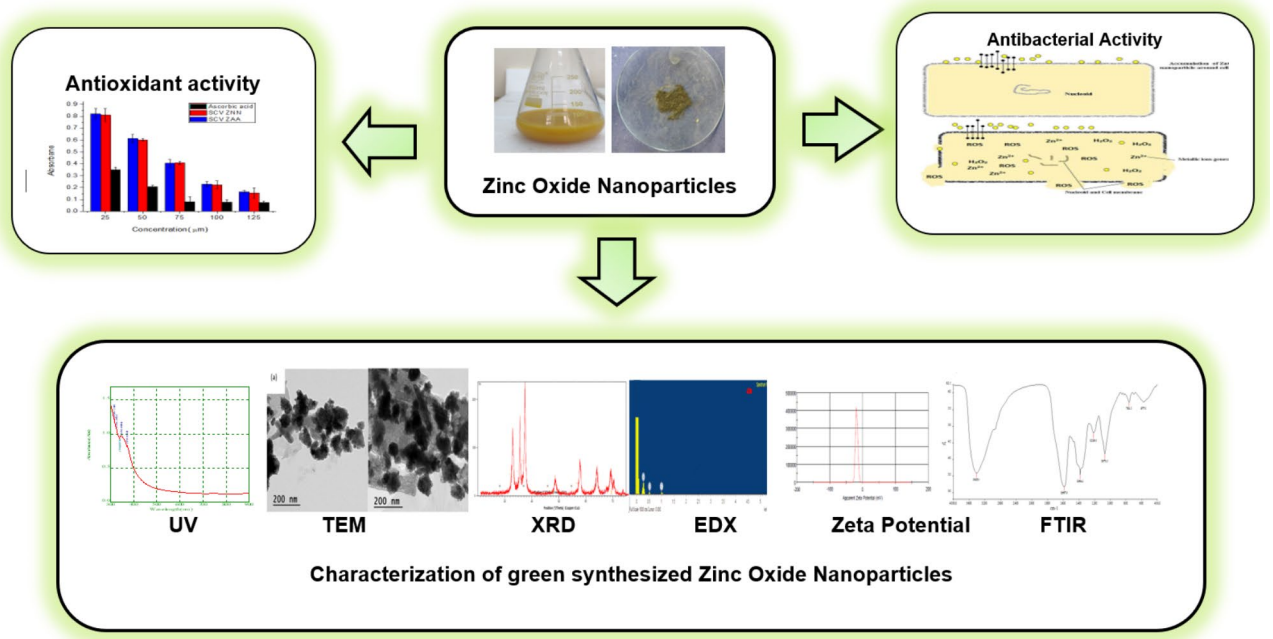

Fig. 2. Pictorial representation of the characterization and biological activities of ZnO NPs via *M. philippinensis*.

	Chemical composition						
	Alkaloids	Saponins	Terpenoids	Tannins	Flavonoids	Glycosidase	Phenol
Result of plant extracts	+	-	+	+	+	+	+

Table 1. Preliminary investigation of phytochemicals in *M. philippinensis* leave extract. Key: + means present and – means absent.

After that, bacterial strains were added to sterilized plates. A loop of bacteria from the prepared slant was dissolved in the necessary amount of distilled water to create a suspension of bacterial strains. 50 µl of the suspension was then loaded onto Muller Hinton Agar plates and gently shifted over the plate surface with a slider. Ultimately, sterilized cork borer was used to create wells with a diameter of 9 mm, into which a micropipette was used to pour the prepared sample solution (100 µg). Following a 24-hours incubation period at 37 °C for each plate, the diameter of the zone of complete inhibition was determined using a ruler scale. The same procedures were used to measure the antibacterial activities of the control (samples without plant extract and ZnO NPs).

Statically analysis

One-way ANOVA was used to analyze variance using Origin 8 software. Each measurement was made three times ($n = 3$), and the standard deviation (SD) and average of the three runs are shown. $P \leq 0.05$ was used to determine significance.

Result and discussion

Upon conducting a phytochemical screening of ethanol extracts from *M. philippinensis*, many compounds were detected, including alkaloids, phenolic groups, steroids, flavonoids, phenols, saponins, sugars, tannins, and triterpenes. Table 1 lists the various phytochemicals found in *M. philippinensis*. This result is similar to the work of Madhavi Adhav[51], who detected that the preliminary phytochemical screening of ethanolic extract reveals the presence of flavonoids, glycosides, phenolic compounds, tannins, proteins, and amino acids in the fruit part of *M. philippinensis.* The ethanolic extract revealed that *M. philippinensis* also contains significant alkaloids, flavonoids, steroids, saponins, and phenols for their antioxidant and antibacterial activities[52]. The results of different experiments performed for the phytochemical investigations revealed the presence of flavonoids, Glycosides, reducing sugars, phlobatanins, steroids, Tannins, anthraquinones, and Terpenoids were also present in *M. philippinensis*[53].

UV-vis spectrum

ZnO nanoparticles' optical characteristics were examined using visible and ultraviolet absorption spectroscopy in the 280–800 nm range. ZnO nanoparticle generation was observed visually; the formation of ZnO

nanoparticles is shown by the color change from white at the beginning to yellow at the end. Figures 1 and 2 show the synthesized nanoparticles' absorbance spectra using zinc nitrate and zinc acetate as zinc sources. Additionally, ZnO production was validated using UV-Vis measurements. According to the data of UV-visible absorption investigations, the generated nanoparticles utilizing zinc nitrate as the zinc source samples had a significant absorption peak at λmax = 365–393 nm in the UV-visible spectrum. This finding is confirmed by the work of Sharmila et al.[15], who examined the ability of *T. castanifolia* to synthesize ZnO NPs. The maximum absorbance peak was obtained at 380 nm. Similar results of absorption peak obtained for ZnO NPs at 370 nm were reported by Padalia and Chanda[54]. The UV-vis data showed that the presence of bioactive compounds such as alkaloids, terpenoids, tannins, flavonoids, glycosidases, and phenol are responsible for ZnO NPs synthesis. This is supported by Mittal et al.[55]; Their result confirmed that phytochemicals such as alkaloids, terpenoids, phenolics, flavonoids, and polypeptides present in the *T. castanifolia* leaf extract act as reductant, which plays a significant role in the ZnO NPs formation. In addition, Abdelbaky et al.[13], confirm green synthesized ZnO NPs mediated by *P. odoratissimum* using UV-Vis spectrophotometry. Their result indicated the formation of ZnO NPs at absorbance peak of 370 nm. The UV-Vis spectrogram of the generated nanoparticles employing zinc acetate as the zinc source showed a broad absorption peak at λmax = 343–347 nm (Fig. 2), confirming the presence of ZnO nanoparticles that may be attributed to the ZnO nanoparticles. This result is confirmed in the work of Nozipho et al. (2024)[7]. Based on their result at a maximum absorption peak of 350 nm, the formation of ZnO NPs mediated by *Mucuna pruriens* was confirmed. The differences in the crystallite sizes of the samples resulting from varying ZnO NP concentrations cause these discrepancies in the absorbance bands of the samples[56]. These peaks result from an electron traveling from ZnO's basic band gap absorption (O2p → Zn3d) to the conduction band[57]. A Tauc plot of the absorbance data for each sample calculates the energy gap[58]. The predicted energy band gap of the ZnO nanoparticles made using zinc acetate was 3.57–3.61 eV, which is greater than the result achieved with zinc nitrate sources (3.50). This is due to different reasons such as the synthesis method, the purity of the starting materials, and the presence of impurities or defects in the synthesized ZnO material. Impurities in the raw materials may cause variations in the band gap energy of the produced ZnO. The method utilized to make zinc nitrate or zinc acetate can impact the band gap energy of zinc oxide. In general, both Figs. 3 and 4 show the distinctive absorption peak of ZnO at around 370. Electron transfers from the valence band to the conduction band (O2p–Zn3d) are responsible for ZnO's inherent band gap absorption[59,60]. Numerous biological characteristics, including antioxidant and antibacterial properties, can be linked to this bandgap[61].

X-Ray diffraction (XRD) analysis

By measuring the interatomic distance and angle as well as the way atoms are arranged in crystalline solids, XRD can be utilized to ascertain the structure of these materials[62]. The XRD pattern of the synthesized zinc oxide nanoparticles (ZnO NPs) in Figs. 5 and 6 clearly shows the crystalline structure of the leaf-based ZnO nanoparticles, which were prepared utilizing zinc nitrate and zinc acetate as precursors. Six separate diffraction peaks were visible in the XRD pattern, as seen in Fig. 5, at degrees 32.519, 34.380, 36.487, 47.810, 56.737, and 62.727. Figure 6 also showed interesting XRD peaks at 32.837, 32.962, 36.514, 47.712, 56.921 and 63.230 degrees. The synthesized nanoparticles' hexagonal wurtzite structure was verified by indexing these peaks with

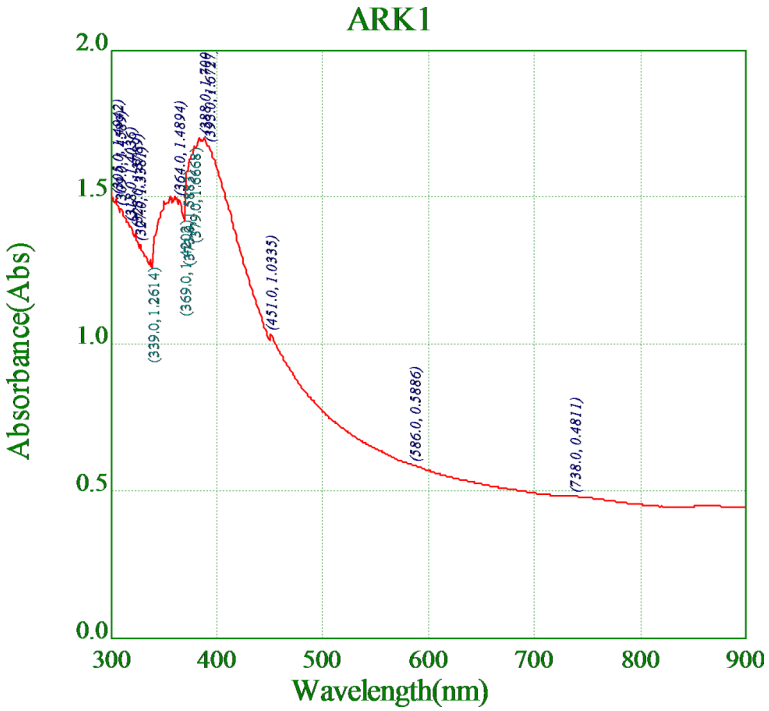

Fig. 3. UV-vis spectrogram of synthesized nanoparticles using zinc nitrate as zinc source.

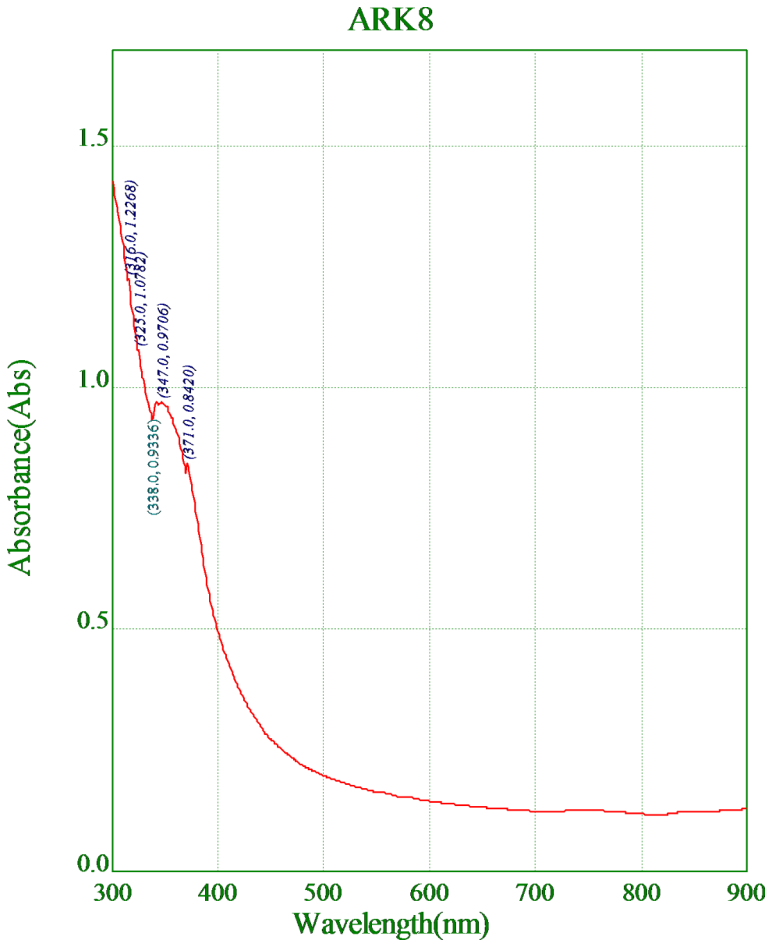

Fig. 4. UV-vis spectrogram of synthesized nanoparticles using zinc acetate as zinc source.

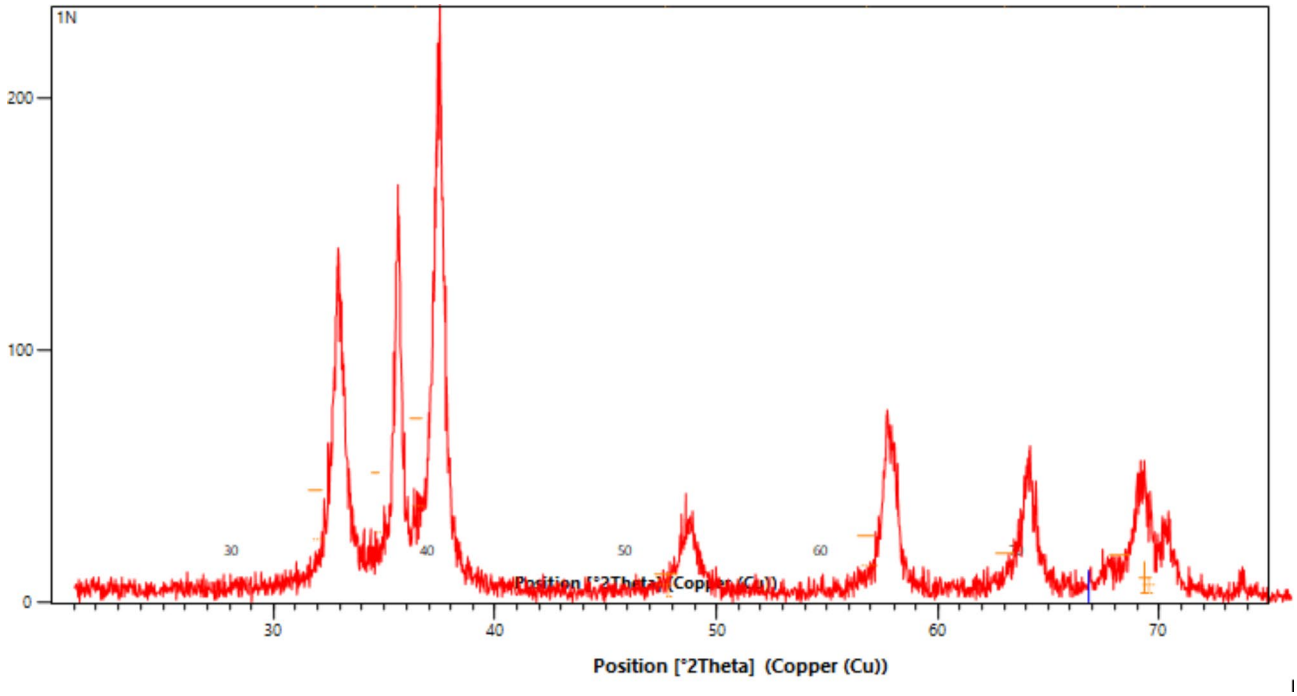

Fig. 5. XRD spectrogram of synthesized nanoparticles using zinc nitrate as zinc source.

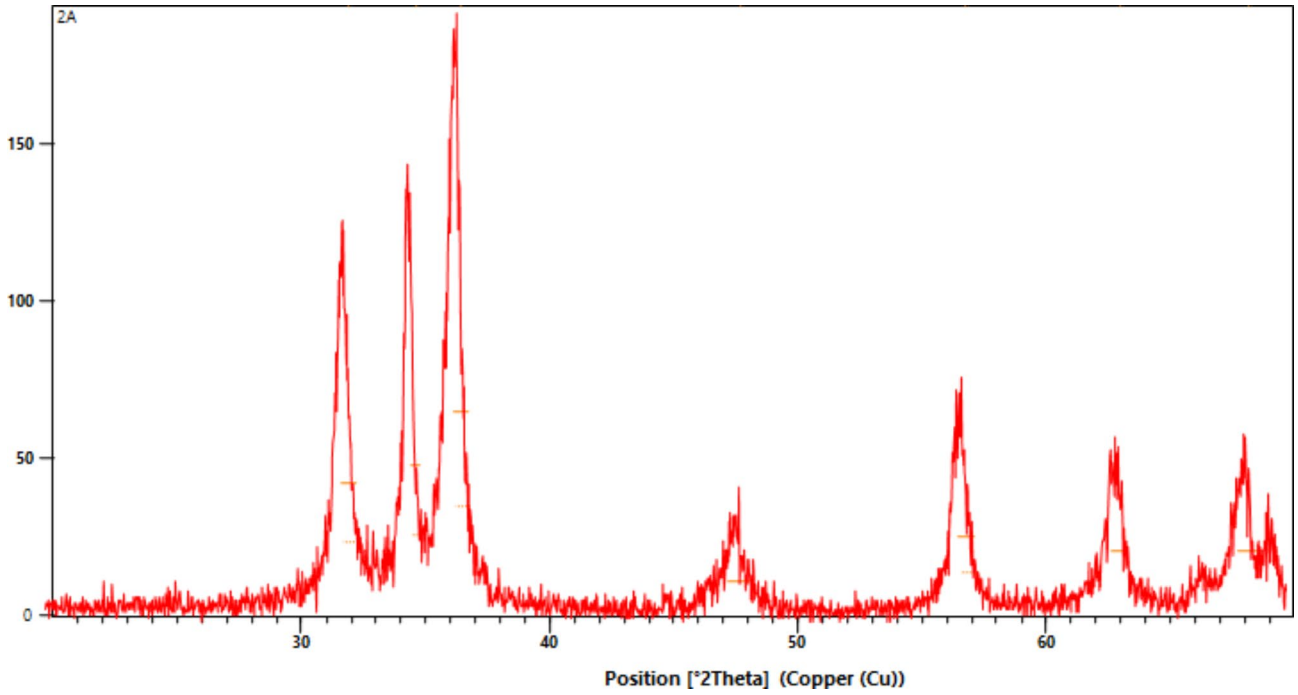

Fig. 6. XRD spectrogram of synthesized nanoparticles using zinc acetate as zinc source.

the corresponding diffraction lattice planes, hkl value of (100), (002), (101), (102), (110), (103), and (112). This outcome aligns with JCPDS card number 36-1451 from the Joint Committee on Powder Diffraction Standards[63]. The largest intense peak (101) was used to calculate the average size of ZnO NPs using the Debye-Scherer Eq. 2. For the generated ZnO NPs, the average crystallite size was determined to be 21 nm and 28 nm for zinc nitrate and zinc acetate as precursor. The produced ZnO NPs' particle size closely matched earlier observations[64,65]. The ZnO NPs produced using both techniques display comparable peak intensity profiles with little shifts in peak positions, indicating a hexagonal wurtzite structure.

Transmission electron microscopy

Transmission electron microscopy (TEM) spectroscopy was used to examine the surface morphology of the generated ZnO NPs. Using zinc nitrate and zinc acetate solutions, TEM pictures of ZnO NPs demonstrated that they were irregular in shape, with sizes less than 21.25 nm and 36.12 nm, respectively (Fig. 7a and b). Compared to other TEM analyses, Al-Askar et al.[66] got a spherical and smaller average size of ZnO NPs (12.0 nm) using the *P. indica* plant. However, a higher average size (46.6 nm) with an irregular shape was obtained by Mishra et al.[67]. The shape and size of ZnO NPs biosynthesized agree with several other studies[68,69].

Energy dispersive x-ray (EDX) analysis

The composition of the nanoparticles was determined using EDX. Figure 8a,b show sharp signals at 1 keV and 0.5 keV corresponding to Zn and O, respectively, thus showing the formation of ZnO NPs. The presence of bioactive components in plant extract could explain the other signals observed in the spectrum.

Fourier transform infra-red (FT-IR) analysis

FT-IR is used to identify the various functional groups present in the sample because absorption modifies the rotational and vibrational states of molecules and because different functional groups absorb various infrared light frequencies[70]. The FT-IR spectra of the powder ZnO nanoparticle samples showed multiple unique peaks.

The presence of an O-H stretch band for both zinc nitrate and zinc acetate-mediated ZnO NPs corresponds to the O-H stretching of alcohol, phenolic compounds, and flavonoid components, as indicated by the broad stretch peak at 3410 cm^{-1} and 3340.6 cm^{-1} in Fig. 9a and b[71,72]. The low-intensity bands found at 2923 cm^{-1} and 2920 cm^{-1} were due to -CH stretching vibration of the hydroxyl compounds[73]. The peaks around 1600 cm^{-1} confirm the stretching C = C vibration of the aromatic ring system[74]. The C-O stretching bond of the aromatic rings is responsible for the significant intensity peaks at 1071.2 cm^{-1} and 1067 cm^{-1}. Flavonoids and Phenols present in the leaves of *M. philippinensis*, as shown in Table 1, may also be connected to these peaks. The low intense band around 761.5 cm^{-1} and 761.3 cm^{-1} is due to the -CH stretching vibration of aromatics ring[63]. Other peaks at 1557.00 cm^{-1}, 1384.00 cm^{-1}, 1354.8, 1215.60 cm^{-1}, and 1204.2 cm^{-1} revealed the C = O frequency of highly conjugated systems, C = C aromatic stretching, and C-O stretching of ArOH, respectively in both zinc nitrate and zinc acetate mediated ZnO NPs. However, the peaks located between 761.5 cm^{-1} and 761.3 cm^{-1} could probably be due to the C–H stretching of alkane in extract[75]. Finally, the peaks located between 577 cm^{-1}

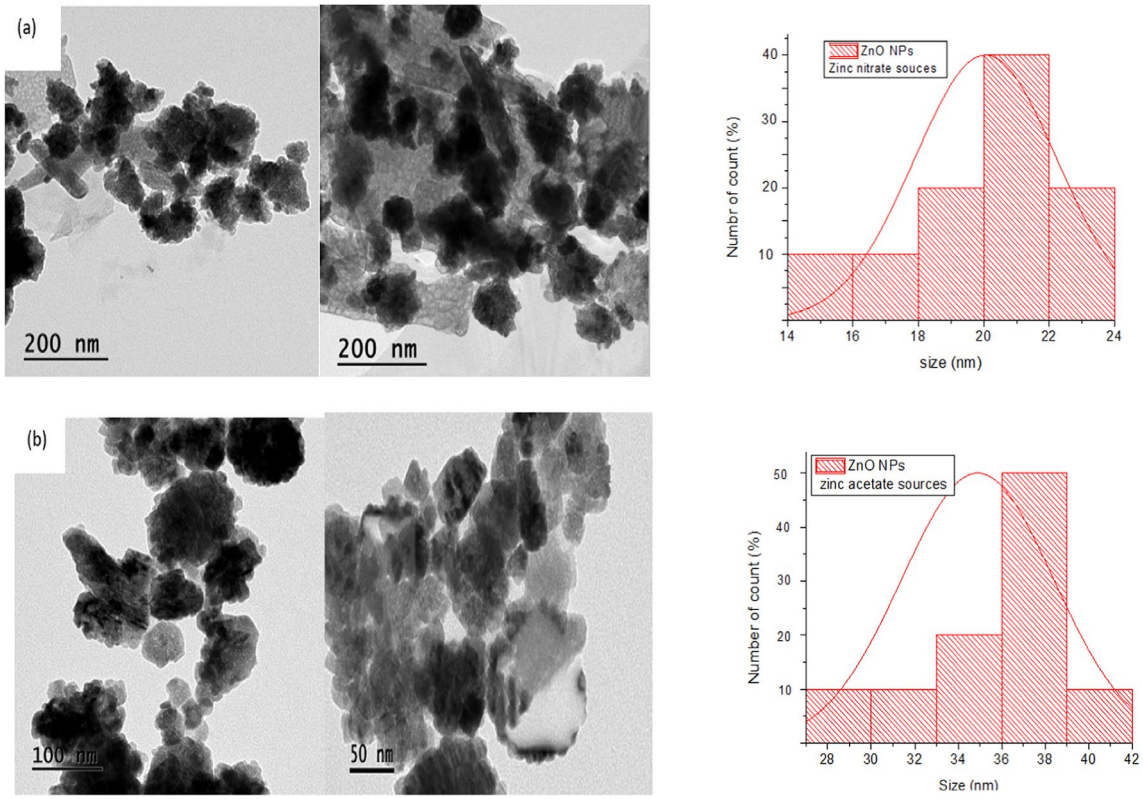

Fig. 7. TEM image of synthesized nanoparticles using zinc nitrate (**a**) mediated nanoparticles and zinc acetate mediated nanoparticles (**b**) and their size distribution to the right of each TEM image.

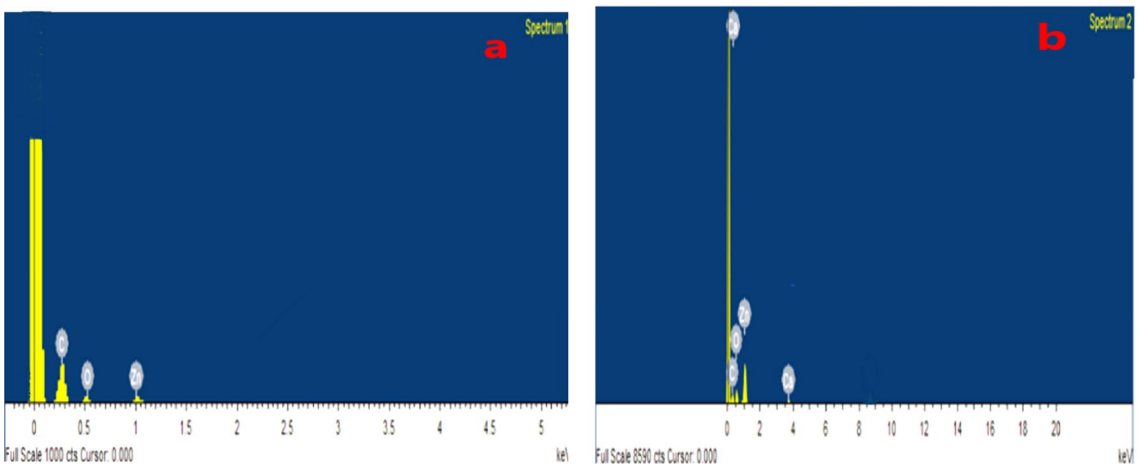

Fig. 8. EDX spectrum of synthesized nanoparticles using zinc nitrate (**a**) mediated nanoparticles and zinc acetate mediated nanoparticles (**b**).

and 583.4 cm^{-1} for the synthesized nano ZnO samples could probably be assigned to the stretching of Zn–O bonds. A similar peak range was also associated with Zn–O bonds, as reported by Santhoshkumar et al.[76].

As observed in the FTIR peaks, nearly identical functional groups such as hydroxyl groups, C = O frequency of widely conjugated systems, C = C aromatic stretching, and C-O stretching of ArOH, are present in both samples (Fig. 9a,b) in high intensity. Therefore, the zinc oxide nanoparticles' FTIR spectra demonstrated that more bioactive compounds are present in charge of capping and stabilizing the ZnO nanoparticles. There is little difference in intensity peaks of Fig. 9a,b due to the difference in the synthesis method, the purity of the starting materials, and the presence of impurities or defects in the synthesized ZnO material. Impurities in the raw materials may cause variations in the intensity of the band.

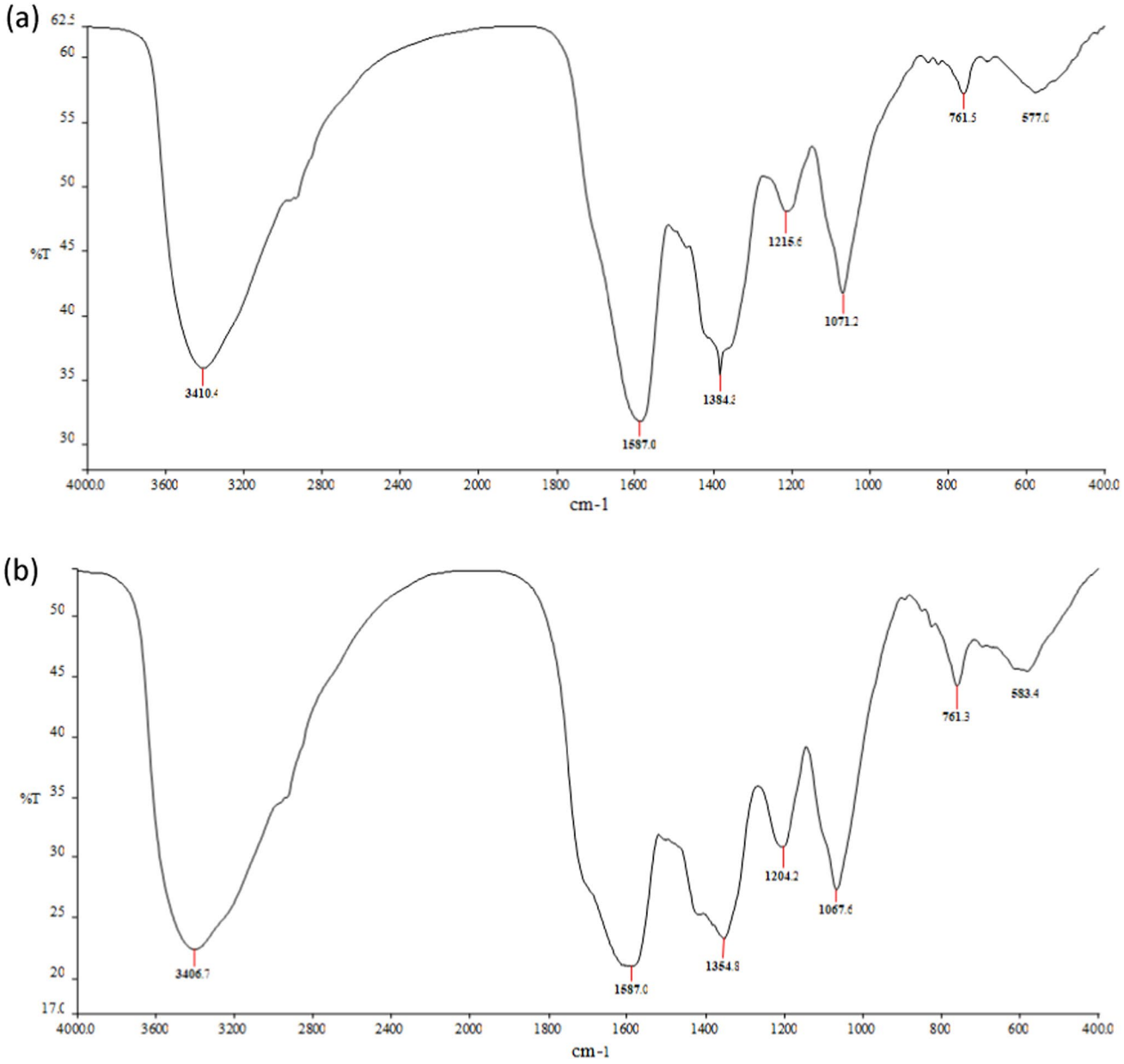

Fig. 9. FTIR spectra of leaf extract mediated nanoparticles from zinc nitrate mediated nanoparticles (**a**) and zinc acetate mediated nanoparticles (**b**).

Stability of ZnO NPs

The surface charges and stability of biosynthesized ZnO NPs have been assessed through zeta potential (ZP) analysis as observed in Fig. 10a and b. When examining the NP surface charge and colloidal stability, zeta potential (ZP) is a crucial parameter. ZnO NPs have a zeta potential of – 18.1 mV and – 18.1 mV for both zinc nitrate-mediated nanoparticles (Fig. 10a) and zinc acetate-mediated nanoparticles (Fig. 10b), indicating that they form stable ZnO NPs at basic pH (8.1). A comparable zeta potential of -19.3 mV indicates the stability of ZnO NPs[77]. As a result, the reducing agents (i.e., phenolic and flavonoid components) found in the leaf extract (LE) (Table 1) are probably responsible for the negative charge potential of the produced ZnO NPs.

Application of synthesized ZnO nanoparticle

Antioxidant activities

Antioxidants donate electrons to free radicals and mask their harmful effects on biological processes to reduce oxidative damage. The antioxidant activity of the particles was determined by assessing the green-synthesized ZnO NPs' capacity to scavenge free radicals produced by DPPH and detecting the decrease in DPPH absorbance at 517 nm wavelength. In DPPH free radical, antioxidant compounds can take hydrogen atoms or electrons from the DPPH radical, which has a violet color, and reduce it to DPPH-H (yellow color). The scavenging activity of the produced ZnO is evaluated by monitoring the DPPH's color change using spectrophotometry.

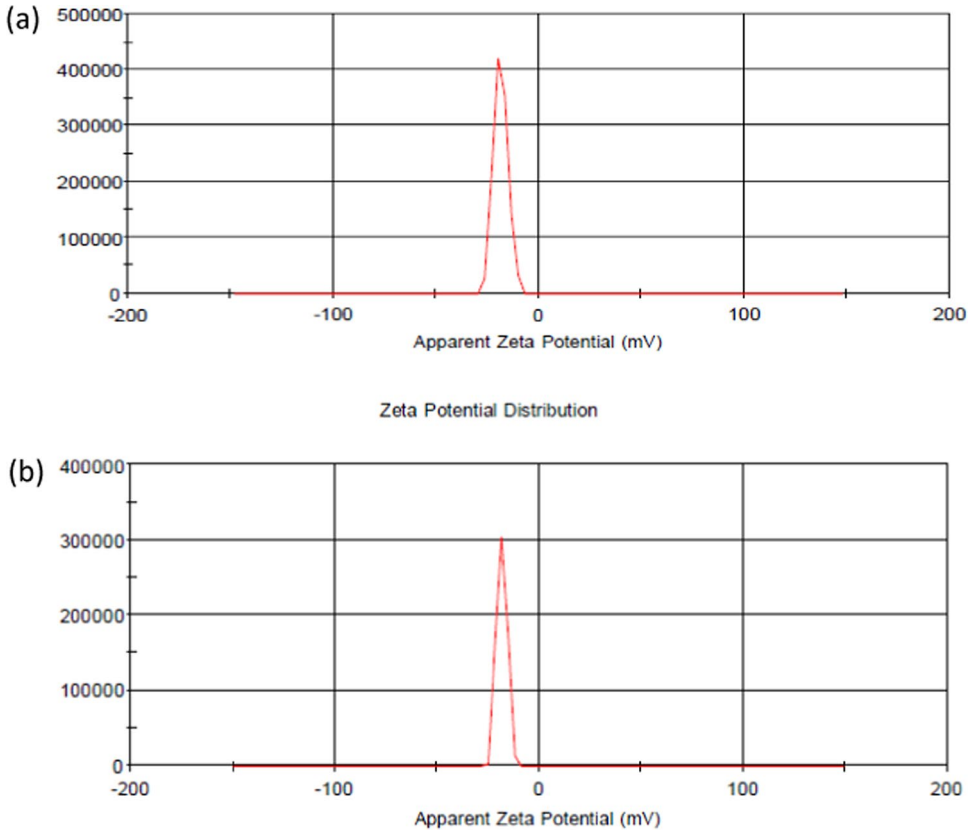

Fig. 10. Zeta potential value of ZnO NPs formed due to zinc nitrate (**a**) and zinc acetate (**b**) precursor.

The color change from blue to yellow confirmed the antioxidant capacity of the nanoparticles[7]. DPPH radicals are a frequently used model system to study the ability of various natural or phytochemicals to scavenge free radicals[23].

The antioxidant activity of ZnO NPs mediated by *M. philippinensis* and ascorbic acid is shown in Fig. 12. The results show that the antioxidant experiment conducted on nanoparticles reveals significant antioxidant capacity. The ZnO NPs' DPPH activity increased in a dose-dependent manner. The ZnO NPs concentrations that scavenged the DPPH radical rose from 25 to 125 µg. For the nanoparticles made from *M. philippinensis* leaf extract and zinc nitrate, the percentage of DPPH radical inhibition ranged from 18.82%± 0.40 (25 µg concentration) to 84.05% ± 0.38 (125 µg concentration). In contrast, for the nanoparticles made from *M. philippinensis* leaf extract and zinc acetate, DPPH radical inhibition ranged from 16.45%±0.71 (25 µg concentration) to 83.13% ±0.22 (125 µg concentration). For ascorbic acid scavenging activities at 125 µg concentration, the highest value of 92.24%± 0.63 was observed compared to both zinc nitrate-mediated nanoparticles (84.05%±0.38) and zinc acetate-mediated nanoparticles (83.13% ±0.22). As observed in error bar in Fig. 11 there was no significant difference ($P > 0.05$) (in DPPH scavenging activities between 75, 100 and 124 µg concentrations in ascorbic acid (Fig. 11). There is no significant different between the scavenging activities between two sample (SCVZNN and SCVZAA) at 100 and 125 µg concentration.

As observed in Fig. 12, ZnO NPs had superior inhibitory efficiency in the DPPH scavenging assay compared to the reference chemical, ascorbic acid.

The absorbance at 517 nm changed when ZnO NPs were added to the DPPH solution (Fig. 11). For both samples, the maximum intensity at 517 nm gradually reduced with time in agreement with changes in color of the DPPH solution in the presence of ZnO NPs. The drop in peak intensity proved that ZnO nanoparticles could scavenge free radicals because ZnO NPs scavenge DPPH by donating a hydrogen atom to stabilize the DPPH molecule[78]. The plant mediated ZnO NPs and ascorbic acid effectively prevented the DPPH with the IC_{50} value ranging from 60 to 67 µg/ml. The smallest IC_{50} value was observed for ascorbic acid with a 60.07 µg/ml value. The IC_{50} value of the nanoparticles mediated by zinc nitrate and leaf extract was determined to be 65.31 µg/ml. In contrast, the nanoparticles generated from zinc acetate had an IC_{50} value of 66.87 µg/ml; this showed that Zinc nitrate-mediated nanoparticles demonstrated the highest level of antioxidant activity compared to zinc acetate-mediated nanoparticle type because the lower the IC_{50} values, the higher the antioxidant activities. The difference in the value of IC_{50} occurred due to the difference in the size between them. The higher antioxidant activities of the first compared to the second is due to the difference in the size between them. The active phytochemicals of *M. philippinensis*, including steroids, flavonoids, alkaloids, saponins, phenols, glycosides, and tannins (Table 1) have been reported to act as bio-reductants. Many studies have specified that various OH groups' presence in phenolic and flavonoids are responsible for the formation and stabilization of metal oxide

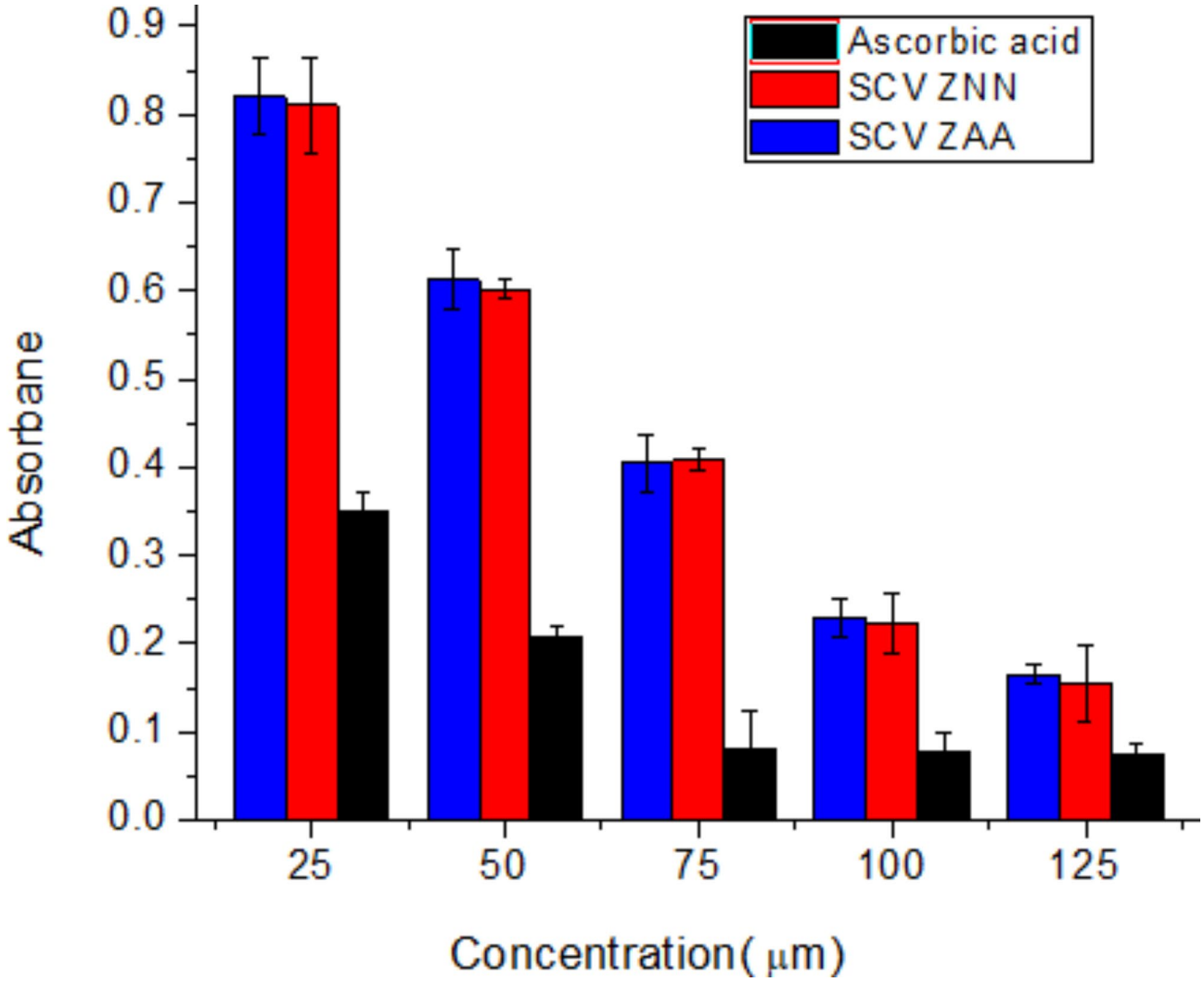

Fig. 11. The absorbance of synthesized ZnO NPs from leaf extracts of *M. Philippines* and ascorbic acid (SCVAA), zinc acetate-mediated nanoparticles (SCVZAA), and zinc nitrate-mediated nanoparticles (SCVZNN) after added to DPPH.

nanoparticles[79]. Additionally, the phytochemicals in *M. philippinensis* are capped over ZnO NPs, can donate hydrogen, and give ZnO NPs a strong antioxidant potential[80].

A number of researchers reported similar results of ZnO NPs by DPPH radical scavenging; for instance, in the work of Shnawa et al.[28], in comparison to vitamin C, *Z. spina-christi* mediated ZnO nanoparticle showed promising H_2O_2 and DPPH free radical scavenging properties. Alghamdi et al.[29] showed the powerful radical scavenging activity of *C. argentea* mediated ZnO NPs with an Ic_{50} value of 91.24 mg/ml comparable to well-known standard chemicals such as ascorbic acid (Ic_{50} = 14.37 mg/ml). By employing aqueous extracts of *A. sativum*, *R. officinalis*, and *O. basilicum*, Stan et al.[81] produced ZnO NPs by a combination of biological and chemical methods (coprecipitation). An analysis was conducted to determine how plant extract affected the antioxidant capabilities of green-produced nanoparticles. The result showed that ZnO NPs synthesized using extracts of the selected plant species were found to exhibit more antioxidant activities than chemical ZnO NPs.

Antibacterial activity

The biosynthesized ZnO nanoparticles' antibacterial activity against Gram-positive (*S. aureus* and *S. pneumoniae*) and Gram-negative (*K. pneumoniae* and *E. coli*) bacteria was assessed using the disc-diffusion method, with saline acting as a negative control.

Nanoparticles synthesized from zinc sources, such as Zinc nitrate and Zinc acetate, showed excellent antimicrobial potential against both Gram-positive and negative bacteria species. The maximum zone of inhibition when zinc nitrate was used as a zinc source was reported in *S. pneumonia* (14.97 ± 0.38 mm), and the minimum zone of inhibition was reported in *E. coli* (14.10 ± 0.40) (Table 2). Zinc acetate-based ZnO NPs in the same concentration showed the maximum (13.89 ± 0.44) and minimum (13.31 ± 0.39) zone of inhibitions for the *S. pneumonia* and *E. coli*, respectively. Zinc nitrate-mediated ZnO NPs in *M. philippines* do not significantly differ ($p > 0.05$) in their antibacterial activities from gram-positive bacteria like *S. aureus* and *S. pneumonia*; however,

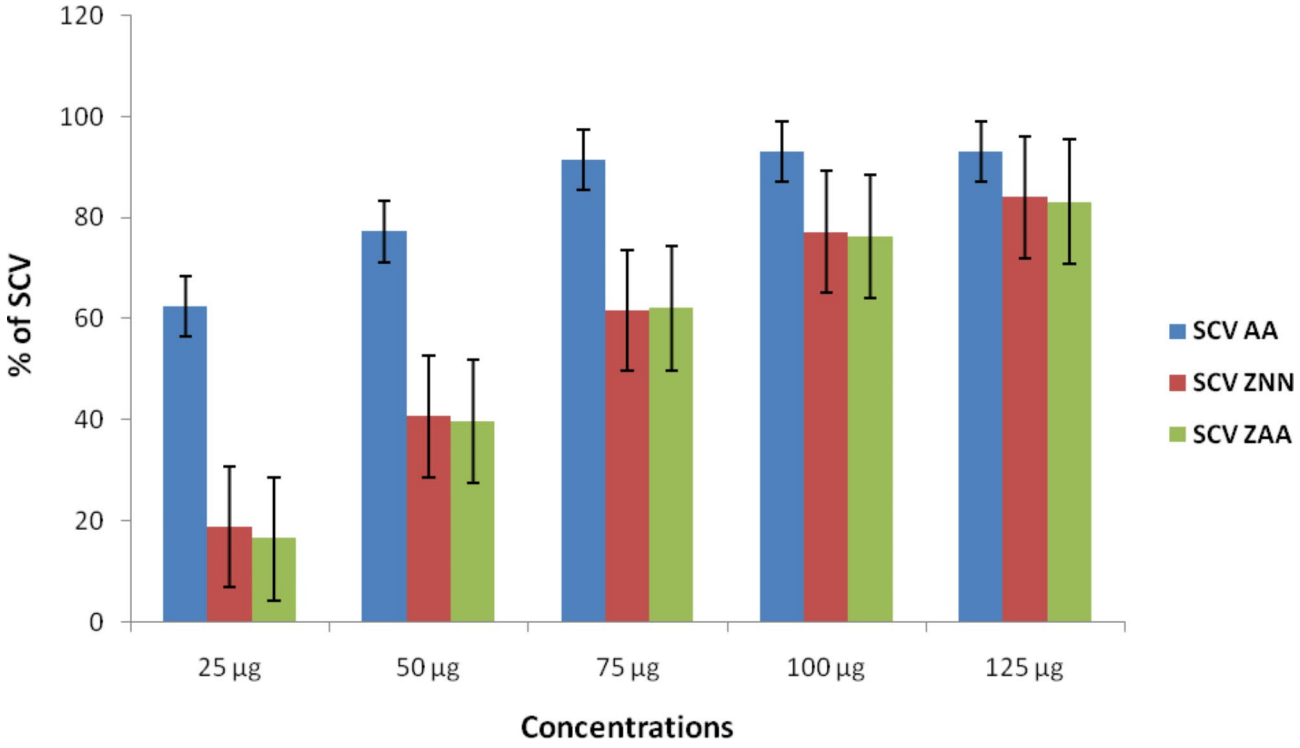

Fig. 12. DPPH radical scavenging activity of synthesized ZnO nanoparticles from leaf extracts of *M. Philippines* (SCVAA = scavenging activity of ascorbic acid; SCVZNN = scavenging activity of zinc nitrate-mediated nanoparticles and SCVZAA = scavenging activity of zinc acetate-mediated nanoparticles).

ZnO NPs sample	Concentration	Test organisms				
		Control	Gram positive		Gram negative	
			S. aureus	*S. pneumoniae*	*E. coli*	*K. pneumoniae*
M. philippines mediated ZnO NPs using Zinc nitrate	100 µg	0.00	$14.88^{a} \pm 0.36$	$14.97^{a} \pm 0.38$	$14.10^{c} \pm 0.40$	$14.76^{b} \pm 0.79$
M. philippines mediated ZnO NPs using Zinc acetate	100 µg	0.00	$13.58^{a} \pm 0.66$	$13.89^{b} \pm 0.44$	$13.31^{c} \pm 0.39$	$13.46^{d} \pm 0.56$

Table 2. Antimicrobial activity of zinc nitrate and zinc acetate *M. Philippines* based ZnO nanoparticles against different bacterial strains. After examining each data set in triplicate, the mean value ± SD was calculated. The same alphabetical letter (a, b, c, and d) showed that there is no significant difference ($P > 0.05$) between the samples.

gram-negative bacteria like *E. coli* and *K. pneumonia* have statistically significant ($p < 0.05$). In comparison to *M. philippines*-mediated ZnO NPs employing Zinc nitrate sample, the antibacterial activity potential for both gram-positive and gram-negative bacteria is lower in the Zinc acetate-mediated sample. In both *M. Philippines*-mediated tests, zinc nitrate and zinc acetate-synthesized ZnO NPs demonstrated greater antibacterial activity against Gram-positive bacterial strains than Gram-negative bacterial strains. Furthermore, ZnO nanoparticles were shown in a prior study to have greater bactericidal activity against Gram-positive bacteria than Gram-negative bacteria[82]. The results agree with the early literature and findings of many other workers. ZnO-NPs produced by *Z. spina-christi* demonstrated strong antibacterial activity against the tested bacteria with varying susceptibilities as a concentration-dependent effect. Gram-positive bacteria like *S. aureus* showed a larger zone of inhibition (36 mm) when ZnO-NPs were applied at the same dose than gram-negative bacteria like *E. coli* (15 mm)[28]. Utilizing the agar disc diffusion method, Alghamdi et al.[29] investigated the antibacterial activity against gram-positive and gram-negative bacteria utilizing ZnO NPs mediated by *Celosia argentea*. Their results showed that gram-positive strains harboring biogenic ZnO NPs have a larger bactericidal effect than gram-negative strains in a concentration-dependent manner. The physiological makeup of these microbes varies, which could cause the sensitivity discrepancy between Gram-positive and Gram-negative bacteria. Due to gram-

negative bacteria's outer lipopolysaccharide barrier, antibacterial chemicals cannot penetrate their cell walls. However, they are more vulnerable because gram-positive bacteria only have an exterior peptidoglycan layer—which is ineffective as a permeability barrier. Because of this, the cell walls of Gram-negative bacteria are more complicated than those of Gram-positive bacteria, acting as a diffusion barrier and lessening the susceptibility of the former to antibiotics[83]. Both the biosynthesized ZnO NPs and the leaf extract from *M. Philippines* showed substantial antibacterial action against strains of Gram-negative (*K. pneumonia* and *E. coli*) and Gram-positive (*S. pneumonia* and *S. aureus*) bacteria, as shown in Table 1.

For the first time Al-Askar et al.(2023)[30] investigate the antibacterial properties of *P. indica* mediated ZnO NPs. The result confirmed that with inhibition zones values of 21.83, 13.0, 14.9, 24.26, 17.0, 20.67, and 19.0 mm, antimicrobial activities carried out against *E. coli*, *P. aeruginosa*, *E. faecalis*, *B. subtilis*, *S. aureus*, *C. albicans*, and *C. neoformans* respectively. Another study evaluated the antibacterial efficacy of ZnO nanoparticles made from a synthetic *T. pratense* flower extract against both clinical and conventional strains of *E. Coli*, *P. aeruginosa*, *and S. aureus*. The results showed that ZnO nanoparticles derived from flower extract of *T. pratense* showed strong antibacterial activity against each strain tested. The results largely confirmed that ZnO's inhibitory effect increased with concentration[84].

Researchers have proposed a few possible bactericidal pathways for how ZnO NPs interact with bacteria. There are theories that smaller NPs release Zn^{2+} due to increased surface reactivity and quicker cell penetration. A fundamental concept underlying antibacterial activities is the liberation of Zn^{2+} from ZnO NPs, which is recognized to hinder several bacterial cell functions, such as active transport, metabolism, and enzyme activity[85]. The Zn^{2+} ions released from ZnO NPs attach and damage the bacterial cell wall. It also breaks the layer of sugars, proteins, and lipids of the bacterial cell membrane. Bacteria may also die due to the disruption of DNA by the attack of Zn^{2+} ions, which inhibits bacterial growth and ultimately leads to cell death. The nanoscale size enhances the material's surface area, increasing antibacterial activities. Additionally, their small size allows for easy entry into cells, leading to cell death[86]. The other proposed antibacterial activity stems from producing reactive oxygen species (ROS), leading to oxidative stress and cell damage or death. ZnO NPs commonly employ ROS generation as an antimicrobial activity (Fig. 13)[87]. Nanoparticles accumulate on the surface of bacterial cell walls, and with the help of various protein channels, they enter the body of bacteria; once they enter, they get activated and start producing metallic ions and ROS (Fig. 13). High ROS production finally destroys the integrity of the cell wall and disrupts the nucleoids of bacterial cells[88,89]. As discussed above, ZnO NPs have the potential to decolonize DPPH to show antioxidant activities. Even though DPPH does not directly kill bacteria, there are situations in which the way antioxidants neutralize DPPH can be linked to antibacterial qualities[90]. Antioxidants have the potential to interact with bacterial membranes, increasing their permeability and allowing cell contents to seep out[91]. Certain antioxidants can stop protective layer formation that protects from antibiotics. Compounds that effectively reduce DPPH may have antimicrobial properties through oxidative stress induction and membrane disruption, among other mechanis[91]. Further, the small size of nanoparticles facilitates their easy and fast transportation, resulting in high production ROS and more nanotoxicity[92]. Another proposed mechanism is the lethal activity of the ZnO NPs due to the attachment of the NPs to the bacterial cell membranes and the accumulation inside the cytoplasm, resulting in damaging the cell membrane integrity and loss of cell contents because of the leakage ending up with cell death[89].

Limitations of the study

In this study, antioxidant activity is performed only by the DPPH free radical scavenging method. Only antibacterial activities are included; the paper does not perform antifungal activities.

Conclusion

The study showed how to synthesize ZnO NPs utilizing a green chemistry strategy with two zinc sources, zinc acetate and zinc nitrate, as well as *M. philippinensis* leaf extract as a reducing and capping agent. Zinc nitrate and zinc acetate were utilized as a sources of zinc oxide nanoparticles. FTIR analyses verified that phytochemicals such as flavonoids, alkaloids, terpenoids, tannins, flavonoids, glycosidase and Phenol were present on the nanoparticle surface. The XRD pattern also indicated the hexagonal pure Wurtzite structure. EDX, TEM, FTIR, and DLS confirmed the formation of NPs with an average size of 21.25 nm and 36.12 nm, respectively, as obtained from TEM analysis. Antioxidant potential was evaluated by DPPH assay. Good SCV was observed for both nanoparticles, with IC_{50} values of 65.31 µg/ml and 66.87 µg/ml for the nanoparticles synthesized from zinc nitrate and zinc acetate as a zinc source. Furthermore, ZnO NPs showed excellent antibacterial effects against gram-positive and gram-negative bacteria species. A strong zone of inhibition against gram-positive and gram-negative bacteria with a maximum value of 14.97 ± 0.38 and 14.76 ± 0.79, respectively. These results confirmed that the synthesized nanoparticle is an effective antioxidant and antibacterial agent and may be used in the food industry, medical industry, or other biological applications. These can be used as a safe and stable alternative to synthetic substances in the fields of pharmaceutical and biomedical research.

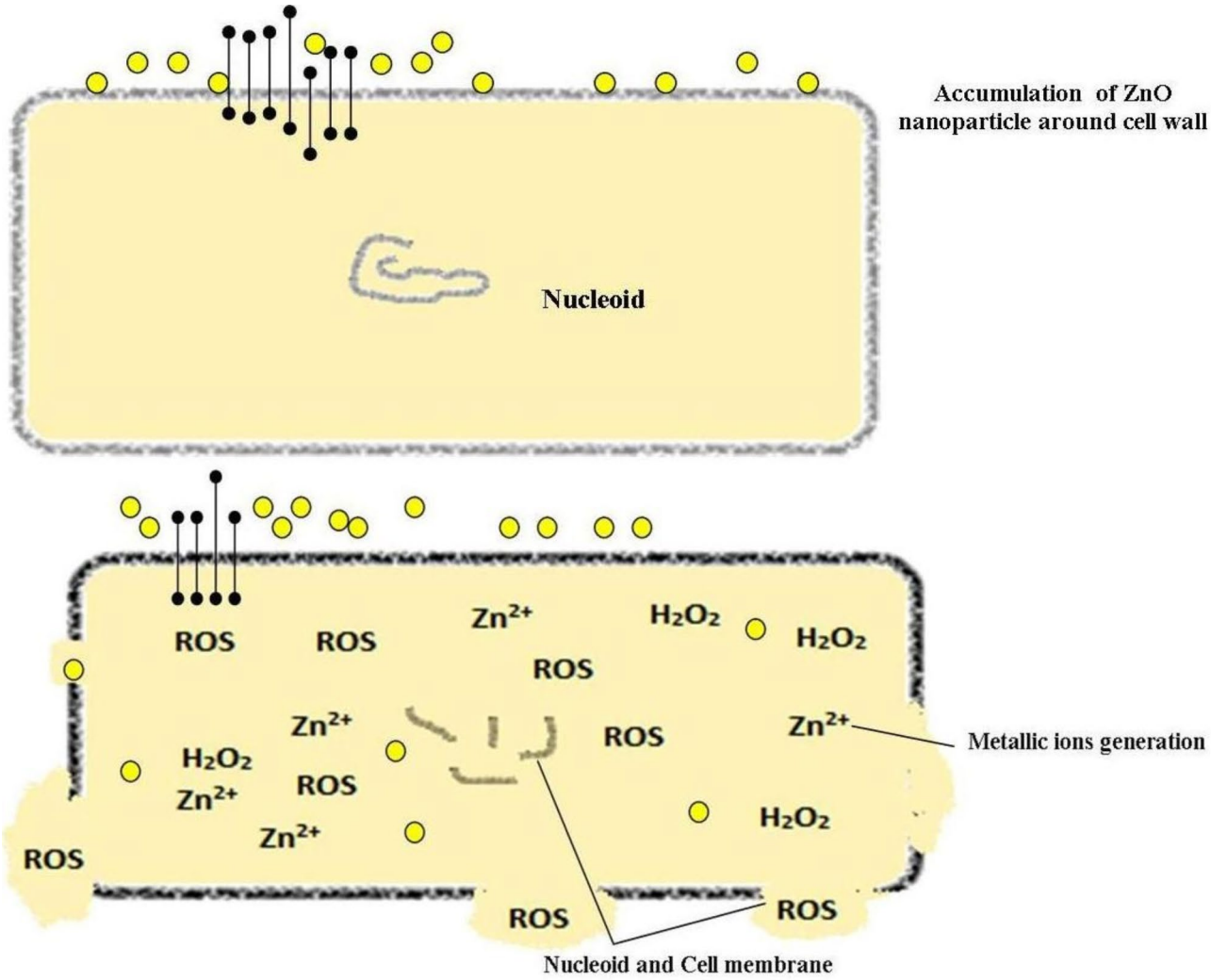

Fig. 13. Possible antibacterial mechanism of synthesized nanoparticle.

Data availability

The data used to support the findings of this study are included within the article.

Received: 4 April 2024; Accepted: 1 January 2025
Published online: 24 February 2025

References

1. Song, J. Y. & Kim, B. S. Rapid biological synthesis of silver nanoparticles using plant leaf extracts. *Bioprocess Biosyst. Eng.* **32**, 79–84 (2009).
2. Hayat, A. et al. Different dimensionalities, morphological advancements and engineering of g-C3N4-based nanomaterials for energy conversion and storage. *Chem. Record* **23**, e202200171 (2023).
3. Ansari, S. A. Elemental semiconductor red phosphorus/ZnO nanohybrids as high performance photocatalysts. *Ceram. Int.* **49**, 17746–17752 (2023).
4. Ansari, S. A. et al. Facile and sustainable synthesis of carbon-doped ZnO nanostructures towards the superior visible light photocatalytic performance. *New J. Chem.* **41**, 9314–9320 (2017).
5. Kandwal, A. et al. Green synthesis, characterization and antimicrobial activity of silver nanoparticles using leaf extract of *Ajuga parviflora* Benth. *Plant. Archives.* **19**, 762–768 (2019).
6. Balgobind, K. et al. Hybrid of ZnONPs/MWCNTs for electrochemical detection of Aspartame in food and beverage samples. *J. Electroanal. Chem.* **774**, 51–57 (2016).
7. Gamedze, N. P. et al. Biosynthesis of ZnO nanoparticles using the aqueous extract of Mucuna pruriens (utilis): Structural characterization, and the anticancer and antioxidant activities. *Chem. Afr.* **7**, 219–228 (2024).
8. Requejo-Isidro, J. et al. Role of surface-to-volume ratio of metal nanoparticles in optical properties of Cu: Al2O3 nanocomposite films. *Appl. Phys. Lett.* **86**, (2005).
9. Cheng, H. et al. Effect of phase composition, morphology, and specific surface area on the photocatalytic activity of TiO2 nanomaterials. *RSC Adv.* **4**, 47031–47038 (2014).
10. Meanwell, N. A. Improving drug candidates by design: A focus on physicochemical properties as a means of improving compound disposition and safety. *Chem. Res. Toxicol.* **24**, 1420–1456 (2011).

11. Jain, K., Mehra, N. K. & Jain, N. K. Potentials and emerging trends in nanopharmacology. *Curr. Opin. Pharmacol.* **15**, 97–106 (2014).
12. Naseem, T. & Durrani, T. The role of some important metal oxide nanoparticles for wastewater and antibacterial applications: A review. *Environ. Chem. Ecotoxicol.* **3**, 59–75 (2021).
13. Abdelbaky, A. S. et al. Green synthesis and characterization of ZnO nanoparticles using *Pelargonium odoratissimum* (L.) aqueous leaf extract and their antioxidant, antibacterial and anti-inflammatory activities. *Antioxidants* **11**, 1444 (2022).
14. Husen, A. & Siddiqi, K. S. Phytosynthesis of nanoparticles: Concept, controversy and application. *Nanoscale Res. Lett.* **9**, 1–24 (2014).
15. Sharmila, G., Thirumarimurugan, M. & Muthukumaran, C. Green synthesis of ZnO nanoparticles using *Tecoma castanifolia* leaf extract: Characterization and evaluation of its antioxidant, bactericidal and anticancer activities. *Microchem. J.* **145**, 578–587 (2019).
16. Soren, S. et al. Evaluation of antibacterial and antioxidant potential of the zinc oxide nanoparticles synthesized by aqueous and polyol method. *Microb. Pathog.* **119**, 145–151 (2018).
17. Zhang, L. et al. Investigation into the antibacterial behaviour of suspensions of ZnO nanoparticles (ZnO nanofluids). *J. Nanopart. Res.* **9**, 479–489 (2007).
18. Ammar, R. B. et al. Antioxidant activity and inhibition of aflatoxin B1-, nifuroxazide-, and sodium azide-induced mutagenicity by extracts from *Rhamnus alaternus* L. *Chemico-Biol. Interact.* **174**, 1–10 (2008).
19. Kumar, S. The importance of antioxidant and their role in pharmaceutical science-a review. *Asian J. Res. Chem. Pharm. Sci.* **1**, 27–44 (2014).
20. Shon, M-Y., Kim, T-H. & Sung, N-J. Antioxidants and free radical scavenging activity of *Phellinus baumii* (phellinus of hymenochaetaceae) extracts. *Food Chem.* **82**, 593–597 (2003).
21. Akbarirad, H. et al. An overview on some of important sources of natural antioxidants. *Int. Food Res. J.* **23** (2016).
22. Salam, H. A., Sivaraj, R. & Venckatesh, R. Green synthesis and characterization of zinc oxide nanoparticles from *Ocimum basilicum* L. var. Purpurascens Benth.-Lamiaceae leaf extract. *Mater. Lett.* **131**, 16–18 (2014).
23. Sonia, S., Ruckmani, K. & Sivakumar, M. Antimicrobial and antioxidant potentials of biosynthesized colloidal zinc oxide nanoparticles for a fortified cold cream formulation: A potent nanocosmeceutical application. *Mater. Sci. Engineering: C.* **79**, 581–589 (2017).
24. Kamo, A. et al. Understanding antibacterial disinfection mechanisms of oxide-based photocatalytic materials. *Nanocomposite Nanohybrid Materials: Process. Appl.* **17**, 195 (2023).
25. Islam, M. F. et al. Green synthesis of zinc oxide nano particles using Allium cepa L. waste peel extracts and its antioxidant and antibacterial activities. *Heliyon* **10**, (2024).
26. Sukri, S. N. A. M. et al. Cytotoxicity and antibacterial activities of plant-mediated synthesized zinc oxide (ZnO) nanoparticles using *Punica granatum* (pomegranate) fruit peels extract. *J. Mol. Struct.* **1189**, 57–65 (2019).
27. Khajuria, A. K., Hano, C. & Bisht, N. S. Somatic embryogenesis and plant regeneration in *Viola canescens* Wall. Ex. Roxb.: An endangered himalayan herb. *Plants* **10**, 761 (2021).
28. Shnawa, B. H. et al. Evaluation of antimicrobial and antioxidant activity of zinc oxide nanoparticles biosynthesized with *Ziziphus spina-christi* leaf extracts. *J. Environ. Sci. Health C Toxicol. Carcinog.* 1–16, (2023).
29. Alghamdi, R. A. et al. Biogenic Zinc oxide nanoparticles from *Celosia argentea*: Toward improved antioxidant, antibacterial and anticancer activities. (2023).
30. Al-Askar, A. A. et al. Green biosynthesis of zinc oxide nanoparticles using *Pluchea indica* leaf extract: Antimicrobial and photocatalytic activities. *Molecules* **28**, 4679 (2023).
31. Furumoto, T. et al. *Mallotus philippinensis* bark extracts promote preferential migration of mesenchymal stem cells and improve wound healing in mice. *Phytomedicine* **21**, 247–253 (2014).
32. Tripathi, I., Chaudhary, P. & Pandey, P. *Mallotus philippensis*: A miracle stick. *World J. Pharm. Res.* **6**, 678–687 (2017).
33. Hussain, A. et al. An account of the botanical anthelmintics used in traditional veterinary practices in Sahiwal district of Punjab, Pakistan. *J. Ethnopharmacol.* **119**, 185–190 (2008).
34. Azam Khan, M., Ajab Khan, M. & Hussain, M. Ethno veterinary medicinal uses of plants of Poonch Valley Azad Kashmir. *Pakistan J. Weed Sci. Res.* **18**, (2012).
35. Kumar, V. P. et al. Search for antibacterial and antifungal agents from selected Indian medicinal plants. *J. Ethnopharmacol.* **107**, 182–188 (2006).
36. Moorthy, K. et al. Phytochemical screening and antibacterial evaluation of stem bark of *Mallotus philippinensis* var. Tomentosus. *Afr. J. Biotechnol.* **6**, (2007).
37. Arfan, M. et al. Antioxidant activity of extracts of Mallotus philippinensis fruit and bark. *J. Food Lipids* **14**, 280–297 (2007).
38. Arfan, M. et al. Antioxidant activity of phenolic fractions. *Czech J. Food Sci.* **27**, 109–117 (2009).
39. Thakur, S. C. et al. An etheral extract of kamala (*Mallotus philippinensis* (Moll. Arg) lam.) seed induce adverse effects on reproductive parameters of female rats. *Reprod. Toxicol.* **20**, 149–156 (2005).
40. Nandhini, V. & Doss, D. Antidiabetic effect of Mallotus philippinensis in streptozotocin induced diabetic rats. *Int. J. Pharma Bio Sci.* **4**, 653–658 (2013).
41. Khan, M. et al. Hexane soluble extract of *Mallotus philippensis* (Lam.) Muell. Arg. Root possesses anti-leukaemic activity. *Chem. Cent. J.* **7**, 1–6 (2013).
42. Nakane, H. et al. Inhibition of HIV-reverse transcriptase activity by some phloroglucinol derivatives. *FEBS Lett.* **286**, 83–85 (1991).
43. Tanaka, R. et al. Potential anti-tumor-promoting activity of 3α-hydroxy-D: A-friedooleanan-2-one from the stem bark of *Mallotus philippensis*. *Planta Med.* **74**, 413–416 (2008).
44. Hong, Q. et al. Anti-tuberculosis compounds from *Mallotus philippinensis*. *Nat. Prod. Commun.* **5**, 1934578X1000500208 (2010).
45. Daikonya, A., Katsuki, S. & Kitanaka, S. Antiallergic agents from natural sources 9. Inhibition of nitric oxide production by novel chalcone derivatives from *Mallotus philippinensis* (Euphorbiaceae). *Chem. Pharm. Bull.* **52**, 1326–1329 (2004).
46. Ramakrishna, S. et al. Effect of *Mallotus philippinensis* Muell.-Arg leaves against hepatotoxicity of carbon tetrachloride in rats. *Int. J. Pharm. Sci. Res.* **2**, 74–83 (2011).
47. Scherrer, P. Nachrichten Von Der Gesellschaft Der Wissenschaften zu Göttingen. *Mathematisch-Physikalische Klasse* **2**, 98–100 (1918).
48. Blois, M. S. Antioxidant determinations by the use of a stable free radical. *Nature* **181**, 1199–1200 (1958).
49. Desmarchelier, C. et al. Antioxidant and prooxidant activities in aqueous extracts of Argentine plants. *Int. J. Pharmacognosy* **35**, 116–120 (1997).
50. Worku, L. A. et al. Experimental investigations on PVA/chitosan and PVA/chitin films for active food packaging using *Oxytenanthera abyssinica* lignin nanoparticles and its UV-shielding, antimicrobial, and antiradical effects. *Int. J. Biol. Macromol.* **254**, 127644 (2024).
51. Adhav, M. Phytochemical screening and antimicrobial activity of *Mallotus philippensis* Muell. *Arg J. Pharmacognosy Phytochem.* **3**, 188–191 (2015).
52. Ali, A. et al. Accessing the medicinal potential of *Mallotus philippensis*: Comprehensive exploration of antioxidant and antibacterial properties through phytochemical analysis and extraction techniques. *Separations* **11**, 165 (2024).
53. Masood Afzal, M. A. et al. Preliminary phytochemical screening and antimicrobial activities of various fractions of *Mallotus philippensis* Muell. (2013).

54. Padalia, H. & Chanda, S. Characterization, antifungal and cytotoxic evaluation of green synthesized zinc oxide nanoparticles using *Ziziphus nummularia* leaf extract. *Artif. Cells Nanomed. Biotechnol.* **45**, 1751–1761 (2017).
55. Mittal, A. K., Chisti, Y. & Banerjee, U. C. Synthesis of metallic nanoparticles using plant extracts. *Biotechnol. Adv.* **31**, 346–356 (2013).
56. Hasan, M. et al. Bioinspired synthesis of zinc oxide nano-flowers: a surface enhanced antibacterial and harvesting efficiency. *Mater. Sci. Eng. C* **119**, 111280 (2021).
57. Zak, A. K. et al. Effects of annealing temperature on some structural and optical properties of ZnO nanoparticles prepared by a modified sol–gel combustion method. *Ceram. Int.* **37**, 393–398 (2011).
58. Johannes, A. Z., Pingak, R. K. & Bukit, M. Tauc plot software: Calculating energy gap values of organic materials based on Ultraviolet-Visible absorbance spectrum. In *Proceedings, IOP conference series: Materials science and engineering*, (IOP Publishing) (2020).
59. Elumalai, K. et al. Bio-fabrication of zinc oxide nanoparticles using leaf extract of curry leaf (*Murraya koenigii*) and its antimicrobial activities. *Mater. Sci. Semiconduct. Process.* **34**, 365–372 (2015).
60. Zak, A. K. et al. Starch-stabilized synthesis of ZnO nanopowders at low temperature and optical properties study. *Adv. Powder Technol.* **24**, 618–624 (2013).
61. Tidjani-Rahmouni, N. et al. Synthesis, characterization, electrochemical studies and DFT calculations of amino acids ternary complexes of copper (II) with isonitrosoacetophenone. Biological activities. *J. Mol. Struct.* **1075**, 254–263 (2014).
62. Khaing, M. M. et al. *Green Synthesis of zinc Oxide Nanoparticles Using Tropical Plants and Their Characterizations* (MERAL Portal, 2018).
63. Alamdari, S. et al. Preparation and characterization of zinc oxide nanoparticles using leaf extract of *Sambucus ebulus*. *Appl. Sci.* **10**, 3620 (2020).
64. Alwan, R. M. et al. Synthesis of zinc oxide nanoparticles via sol–gel route and their characterization. *Nanosci. Nanatechnol.* **5**, 1–6 (2015).
65. Talam, S., Karumuri, S. R. & Gunnam, N. Synthesis, characterization, and spectroscopic properties of ZnO nanoparticles. International Scholarly Research Notices 2012. (2012).
66. Al-Askar, A. et al. Green Biosynthesis of Zinc Oxide nanoparticles using *Pluchea indica* leaf extract: Antimicrobial and photocatalytic activities. *Molecules* **28**, 4679 (2023).
67. Mishra, D. et al. Biosynthesis of zinc oxide nanoparticles via leaf extracts of *Catharanthus roseus* (L.) G. Don and their application in improving seed germination potential and seedling vigor of *Eleusine coracana* (L.) Gaertn. *Adv. Agric.* :1–11, (2023).
68. Sedefoglu, N., Zalaoglu, Y. & bozok, F. Green synthesized ZnO nanoparticles using *Ganoderma lucidum*: Characterization and in vitro nanofertilizer effect. *J. Alloys Compd.* **918**, 165695–165716 (2022).
69. Selim, Y. et al. Green synthesis of zinc oxide nanoparticles using aqueous extract of Deverratortuosa and their cytotoxic activities. *Scienti2c Rep.* **10**, 3445–3449 (2020).
70. Ojeda, J. J. & Dittrich, M. Fourier transform infrared spectroscopy for molecular analysis of microbial cells. *Microb. Syst. Biology: Methods Protocols* 187–211, (2012).
71. Jafarirad, S. et al. Biofabrication of zinc oxide nanoparticles using fruit extract of Rosa canina and their toxic potential against bacteria. *Mechanistic Approach Mater. Sci. Eng. C.* **59**, 296–302 (2016).
72. Awwad, A. M. A. & Ahmad, B. Green synthesis characterization and optical properties of zinc oxide nanosheets using *Olea Europea* leaf extract. *Adv. Mater. Lett.* **5**, 520–524 (2014).
73. El-Belely, E. F. F. et al. Green synthesis of zinc oxide nanoparticles (ZnO-NPs) using Arthrospira platensis (class: Cyanophyceae) and evaluation of their biomedical activities. *Nanomater* **11**, 95 (2021).
74. Yuvakkumar, R. et al. Rambutan peels promoted biomimetic synthesis of bioinspired zinc oxide nanochains for biomedical applications. *Spectrochim Spectrochim Acta Part. Mol. Biomol. Spectrosc.* **137**, 250–258 (2015).
75. Zhang, G., Shen, X. & Yang, Y. Facile synthesis of monodisperse porous ZnO spheres by a soluble starch-assisted method and their photocatalytic activity. *J. Phys. Chem. C* **115**, 7145–7152 (2011).
76. Rajeshkumar, S. et al. Characterization and evaluation of cytotoxic effect, antioxidant and antimicrobial activities of zinc oxide nanoparticles derived from *Justicia adhatoda*. *Appl. Nanosci.* **13**, 3993–4004 (2023).
77. Abdelbaky, A. et al. Green synthesis and characterization of ZnO nanoparticles using *Pelargonium odoratissimum* (L.) aqueous leaf extract and their antioxidant, antibacterial and anti-inflammatory activities. *Antioxidants* **11**, 1444. (2022).
78. Thomas, B., Arul Prasad, A. & Mary Vithiya, S. Evaluation of antioxidant, antibacterial and photo catalytic effect of silver nanoparticles from methanolic extract of *Coleus vettiveroids*—an endemic species. *J. Nanostruct.* **8**, 179–190 (2018).
79. Shafey, A. M. E. Green synthesis of metal and metal oxide nanoparticles from plant leaf extracts and their applications: A review. *Green. Process. Synth.* **9**, 304–339 (2020).
80. Pal, N. et al. Pharmacognostical, phytochemical and pharmacological evaluation of *Mallotus philippensis*. *J. Drug Delivery Ther.* **12**, 175–181 (2022).
81. Stan, M. et al. Antibacterial and antioxidant activities of ZnO nanoparticles synthesized using extracts of *Allium sativum*, *Rosmarinus officinalis* and *Ocimum basilicum*. *Acta Metall. Sin.* **29**, 228–236 (2016).
82. Azam, A. et al. Antimicrobial activity of metal oxide nanoparticles against gram-positive and gram-negative bacteria: A comparative study. *Int. J. Nanomed.* 6003–6009. (2012).
83. Breijyeh, Z., Jubeh, B. & Karaman, R. Resistance of gram-negative bacteria to current antibacterial agents and approaches to resolve it. *Molecules* **25**, 1340 (2020).
84. Dobrucka, R. & Długaszewska, J. Biosynthesis and antibacterial activity of ZnO nanoparticles using *Trifolium pratense* flower extract. *Saudi J. Biol. Sci.* **23**, 517–523 (2016).
85. Huang, Y. et al. Facile synthesis of Zn2+-based hybrid nanoparticles as a new paradigm for the treatment of internal bacterial infections. *Adv. Funct. Mater.* **32**, 2109011 (2022).
86. Kalra, K., Chhabra, V. & Prasad, N. Antibacterial activities of zinc oxide nanoparticles: A mini review. In *Proceedings, Journal of Physics: Conference Series*, (IOP Publishing, 2022).
87. Li, Y., Liao, C. & Tjong, S. C. Recent advances in zinc oxide nanostructures with antimicrobial activities. *Int. J. Mol. Sci.* **21**, 8836 (2020).
88. Lipovsky, A. et al. Antifungal activity of ZnO nanoparticles—the role of ROS mediated cell injury. *Nanotechnology* **22**, 105101 (2011).
89. Sirelkhatim, A. et al. Review on zinc oxide nanoparticles: Antibacterial activity and toxicity mechanism. *Nano-micro Lett.* **7**, 219–242 (2015).
90. Potdar, M. B. et al. An update on the role of antioxidants in health and disease prevention, in *Antioxidants as Nutraceuticals*, 305–336 (Apple Academic, 2025).
91. Ahmed, F. et al. Targeting spore-forming bacteria: A review on the antimicrobial potential of selenium nanoparticles. *Foods* **13**, 4026 (2024).
92. Naqvi, Q-A. et al. Size-dependent inhibition of bacterial growth by chemically engineered spherical ZnO nanoparticles. *J. Biol. Phys.* **45**, 147–159 (2019).

Author contributions

L.A.W., A.K.K., A.K., R.K.S., and R.K.B. all contributed to the first draft of the paper and handled data collecting, analysis, and material preparation. Each author reviewed the completed manuscript and gave their permission. Every contributor contributed to the article's revision as well.

Funding

This research received no specific grant from any funding agency in the public commercial or not-for-profit sectors.

Declarations

Competing interests

The authors declare no competing interests.

Additional information

Correspondence and requests for materials should be addressed to A.K. or L.A.W.

Reprints and permissions information is available at www.nature.com/reprints.

Publisher's note Springer Nature remains neutral with regard to jurisdictional claims in published maps and institutional affiliations.